Chemical Process Design Vol.1 No.1 (2022) 43-58

University of Sistan and Baluchestan

Chemical Process Design

Available online at http://cpd.usb.ac.ir/



A Numerical Investigation of SiC Production from SiO_2 and Carbon in an Industrial Scale

Bahador Abolpour[1,*], Rahim Shamsoddini[2]

[1]Department of Chemical Engineering, Sirjan University of Technology, Sirjan, Iran
[2]Department of Mechanical Engineering, Sirjan University of Technology, Sirjan, Iran

ARTICLE INFO

Article history:
Received: 2022-09-21
Received in revised form: 2022-11-06
Accepted: 2022-11-07
Published online: 2022-11-14

Keywords:
Modeling; Acheson; SiO_2; Carbon; SiC

DOI: *10.22111/CPD.2022.43514.1008*

ABSTRACT

In the present study, a one-dimensional unsteady-state model is developed to investigate an industrial Acheson reactor for producing SiC. The mechanisms of the SiO_2 melting and converting to SiC are investigated using the experimental data of previous works. Additionally, the obtained models are utilized in the developed mathematical model. The finite difference method is used for the simulation of the developed model. The accuracy of the presented model is validated by empirical data. The complete discussions of the reaction progress, melting process, variations of the bed, and also the temperature inside the bed are presented. Attending to the importance of the existing competition between the melting of SiO_2 and converting to SiC, these mechanisms are investigated using the presented data in previous relevant studies and the obtained models are utilized in the developed mathematical model. The model predictions show that the final produced cylinder of SiC at the center line of the reactor occupies 8.05% of the reactor diameter and has 8.16% weight loss during the production process.

1. Introduction

Today, more than 95% of used SiC in the world has been produced in the Acheson process. In this method, SiO_2, as quartz particles, is mixed with carbon, as petrochemical coke particles, with their stoichiometric ratio or with initial carbon more than its ratio. Additive materials such as NaCl, sawdust, organic liquid adhesives, or SiC, have been applied to this initial mixture for improving the properties, such as the bed porosity or heat conductivity, of this solid bed, or decreasing the effects of existing impurities, such as Al (<0.5%), Fe (<0.3%), Mg (<0.25%), Ca (<0.25%) or ash (<5%), based on the required color and quality of the product [1,2]. The required energy for the chemical reaction is provided by passing the electrical power through a graphite element with high electrical resistivity, such as a cylinder or U-shape core or powder of graphite, which is placed in the center of the solid bed [2]. The temperature of this core is about 2000 to 2700^{o}C (attending to the composition of the bed, the type of the used isolate, and extra),

Corresponding author. Tel.: +98 937 806 14 40
E-mail address: bahadorabolpor1363@sirjantech.ac.ir (B. Abolpour).

which can provide the suitable temperature for this reaction (i.e. 1500°C, of course, this reaction can occur at 1200°C at a certain condition of the bed [2]).

Attending to the complexities of the conditions of this bed and also the mechanism of this reaction, there is no numerical investigation on this process, until now. However, there are several experimental investigations in conditions different from the Acheson reactor condition, for obtaining the mechanism of this reaction [6-14]. Nevertheless, there are few empirical studies on the Acheson process [1, 15]. Kumar and Gupta [15] modeled this process using the previously published empirical data of an industrial unit of SiC production [16]. They used a very low-resolution mesh with 500 grids in the radius direction of the reactor and 200-time steps for solving the one-dimensional unsteady state energy equation in a cylindrical reactor with a more than 3 m radii in 40 hr reaction duration. They considered this endothermic reaction as a sink term in this equation, but, ignored the SiO_2 melting process, radiative heat transfer, and also the heat loss from both sides of this reactor. They used a previously presented model for this reaction based on the concentration of CO [1]. Derevyanko and Zhadanos [17] also presented a two-dimensional unsteady state thermo-physical model for the Acheson reactor and solved this model using the finite difference numerical model. The heat convection by diffusion of CO gas inside the solid bed has been considered in this model, but, ignored the SiO_2 melting process, radiative heat transfer, and also the heat loss from both sides of this reactor, are similar to the reference [15]. They only investigated the temperature distribution inside this bed and had no attention to the mechanism of SiC production in this process.

Gupta et al. [32] found that, is industrial scale process can be improved substantially by effectively heating the charge and reducing the radiation losses. Their results were obtained from the laboratory scale hot model study and industrial process of SiC formation. They also presented that heating of the electrode also takes a good amount of heat in the case of an industrial furnace. Alweendo et al. [33] reported a valuable and cost-effective method to synthesize SiC via pyrolysis of rice husk without the use of a catalyst. A tube furnace with various temperatures from 1000°C to 1500°C has been used to pyrolysis rice husk in an Argon atmosphere flowing. They found that pyrolysis temperature has a crucial effect on the SiC process. Feng et al. [34] investigated the forms of the SiC with different particle sizes. The combination of X-ray diffraction (XRD), inductively coupled plasma-atomic emission spectrometry (ICP-OES), scanning electron microscopy (SEM), transmission electron microscopy (TEM), and X-ray photoelectron spectroscopy (XPS) has been used in their study. Their experimental data showed that in SiC powders obtained by the Acheson process, the ingredients of O, Free-Si, Free-C, and Fe impurities are high. Matizamhuka [35] used Fact Sage Software to investigate the dominant reactions occurring during the Acheson process. The effect of impurities, efficiency, and product quality has been considered in their study. Additionally, the effect of varying the SiO_2/C ratio on the composition of the SiC formation reaction.

Raj and Gupta [36] developed a model based on the experimental data for SiC production to measure temperatures in different locations of the furnace. The temperatures of the core and at different radial and angular locations within the furnace have been measured using a ratio pyrometer and thermocouples respectively. They found that the temperature decreased along the radial direction. Raj et al. [37] investigated the progress of SiC formation using the carbothermal route in the Acheson process and hot model study. They used chemical analysis in order to analyze the amount of SiC formation. Their results showed that the temperature measurement at various locations has an important effect on SiC formation. Tanvir Hossain et al [38] presented a method to utilize Si sludge waste by recycling in the presence of C and fabricating SiC with moderate quality. The effects of the mixing ratio of Si and carbon and

synthesis temperature have been considered to determine the optimum condition for obtaining SiC powder. Rao et al. [39] designed a device to measure the core temperature accurately. They studied the effect of relative emissivity of target material and purging gas flow rate on temperature. Their results showed that the relative emissivity of the target material and measuring block thickness have a significant effect on temperature measurement.

In the present study, an industrial reactor for producing SiC is modeled. The driving force for the heat transfer is the temperature gradient in any direction. Attending to the high-temperature difference between the core and the surrounding surface of this cylinder, in the comparison with the temperature gradients in the other directions, the main heat flux in this reactor is in the radial direction. For this purpose, a one-dimensional unsteady-state model is developed considering the heat loss from both sides of the reactor by the radiative and convective heat transfer mechanisms, and also the mechanisms of fusion and chemical reaction. In this model, the properties of the bed and the core of the reactor are varied by temperature and time. The finite difference method is used for the numerical solving of this model. After the mesh study, the prediction of this model is validated using empirical data [16]. Finally, complete discussions from the reaction progress, melting process, variations of the bed, and also the temperature inside this bed are presented. Attending to the importance of the existing competition between the melting of SiO_2 and converting of this component to SiC, it is necessary to investigate the mechanisms of these phenomena. Therefore, first, these mechanisms are investigated using the presented data in previous relevant studies. Then, the obtained models for these mechanisms are utilized in the developed mathematical model.

2. Acheson process description

Based on an old theory, this is a single-stage reaction in the solid phase, as [3, 4]:

$$SiO_2 + 3C \rightarrow SiC + 2CO(g) \quad (1)$$

and produced SiC nucleation is foamed at the surface of the solid carbon [5]. Another theory indicates that this reaction has occurred in the gaseous phase, as [6]:

$$SiO_2 + C \rightarrow SiO(g) + CO(g) \quad (2)$$

$$SiO_2 + CO(g) \rightarrow SiO(g) + CO_2(g) \quad (3)$$

$$C + CO_2(g) \rightarrow 2CO(g) \quad (4)$$

$$2C + SiO(g) \rightarrow SiC + CO(g) \quad (5)$$

However, this reaction produces a porous cylinder of SiC crystals (with 97% quality) around the core of the reactor. First, these crystals have α form and these crystals have been deformed to β shape at temperatures more than 1577°C [2]. The produced gaseous CO during this reaction should diffuse out from this porous solid bed. The average size of SiO_2 and coke particles should be about 6.4mm and 9.5mm, respectively, with a sharp size distribution (with less than 4% fine particles), for having a suitable porosity for diffusing out of this gas [2].

3. Melting mechanism

Based on the Ainslie et al. [18] study on the kinetics of fusion of quartz using the microscopic pethood, this melting process has occurred inhomogeneous until 300°C more than the melting point of the quartz. This process starts from the surface and boundaries of the solid particle and then distributes inside the particle, as an inhomogeneous phase.

They obtained the rate of melting of the quartz as a function of temperature, as seen in Fig. 1. The heat of the phase transition of SiO_2 has been calculated using the HSC software [19] as a function of temperature and has been presented in Fig. 2. As seen in Fig. 2, by increasing the temperature value, the types of this phase transition have been changed and the heat rate of this transition has been increased in semi-linear form but there are a sharp breaking and decrease in the rate of melting at 1983K temperature (SiO_2 melting point). Also, the melting rate remains constant for values above 1983K (as shown in Fig. 1).

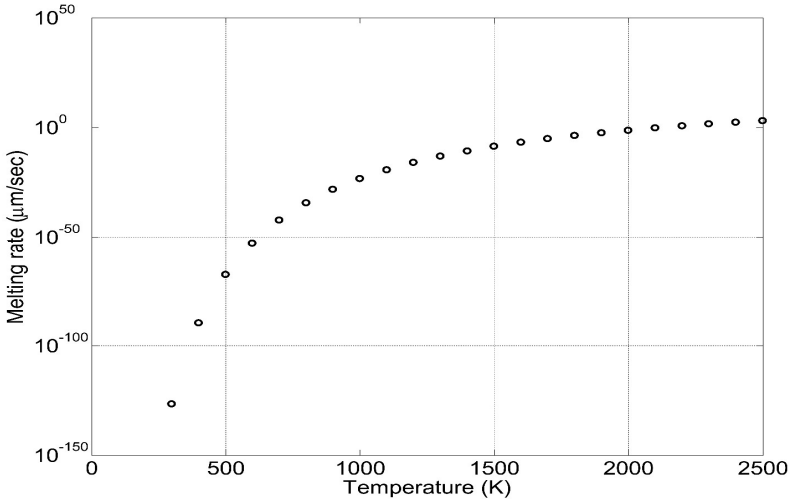


Fig. 1. Rate of melting of quartz [18]

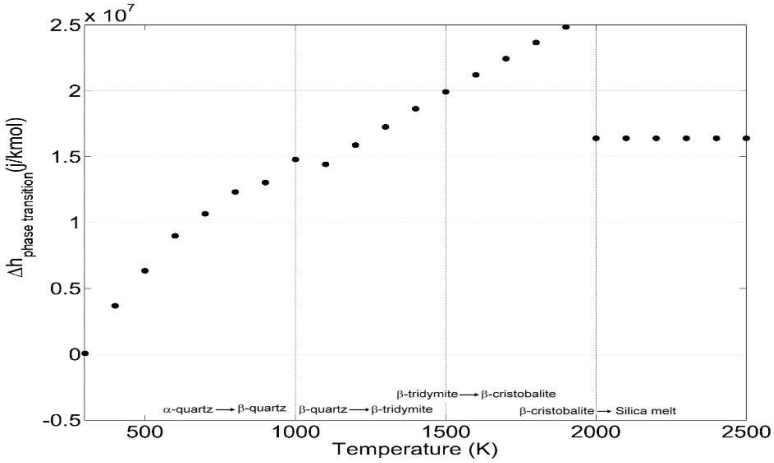


Fig. 2. Heat of the phase transition of SiO_2 [19]

4. Reaction mechanism

It is mentioned that there are different theories relevant to the mechanism of this reaction. The reason for these differences in the definitions of these mechanisms is their assumptions, the calculated activation energy, particle size, the initial ratio of SiO_2 to C, and also the condition of the reaction. The more acceptable mechanism presented for the production of SiC from SiO_2 and Carbon in the Acheson process, which has a low temperature, relatively, is [2]:

$$SiO_2 + C \rightarrow SiO(g) + CO(g) \quad (6)$$

$$SiO_2 + C \leftrightarrow SiO(g) + CO(g) \quad (7)$$

Although some of the other mechanisms presented for this reaction contain Si and CO_2(g) [20], these mechanisms contain the solid penetration, attending to the low diffusion rate of the atoms of Carbon or Si inside the solid phase of SiC or C, have been rejected, previously [20]. Dijon and Metselaar studied the mechanism and also the rate of this reaction [12]. Fig. 3 shows the rate of the conversion of SiO_2 to SiC at different temperatures. Attending to the ability of the nucleation and growth model, as a suitable model for gas-solid reactions [21, 22], presented empirical data in the reference [12] has been fitted to this model for obtaining the parameters of the model (the order of the reaction (n), the activation energy (E) and the pre-exponential factor (k_0)) based on the Arrhenius equation ($k = k_0 \exp(-E/RT)$). Therefore, the following equation, which indicates the progress of this reaction (X) depending on the reaction time (t) based on this model, was fitted with the empirical data of converting SiO_2 to SiC [23]:

$$\left[-\ln(1-X)\right]^n = kt \tag{8}$$

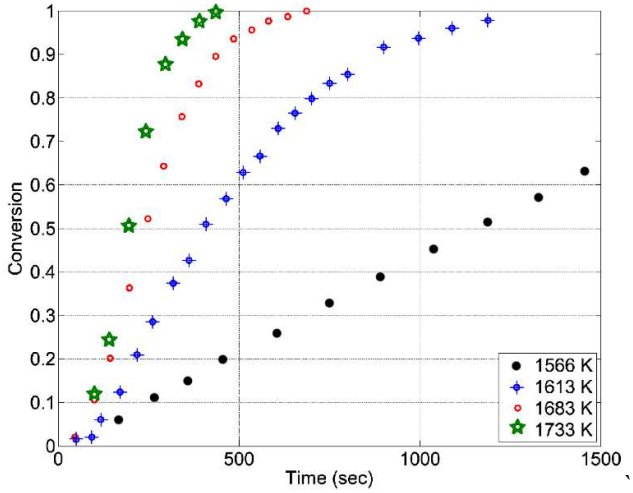


Fig. 3. Rate of the conversion of SiO_2 to SiC [12]

where X and k are SiO_2 conversions and the reaction rate constant respectively. The logarithm form of this equation has been presented below, which shows the linear relation between ln(t) and ln[-ln(1-X)] with a slope equal to n and the width of origin equal to –ln(k):

$$\ln(t) = n\ln\left[-\ln(1-X)\right] - \ln(k) \tag{9}$$

Fitting different lines, with different slopes and widths of origin, on the logarithm form of the presented experimental data in Fig. 3, obtains the order of this reaction, which is equal to 0.512 (as the average of the calculated values for this parameter). Then, fitting different lines, with this slope and different widths of origin, on this experimental data obtains the rate constant of this reaction in different temperatures. Finally, fitting the Arrhenius equation on these rate constants obtains the activation energy of this reaction equal to -251.083kJ/mol, which is near to the obtained values in the previous studies [12], and the pre-exponential factor equal to 2.03×105(1/sec). The heat of this reaction was obtained using the HSC software [19] as a function of temperature (see Fig. 4).

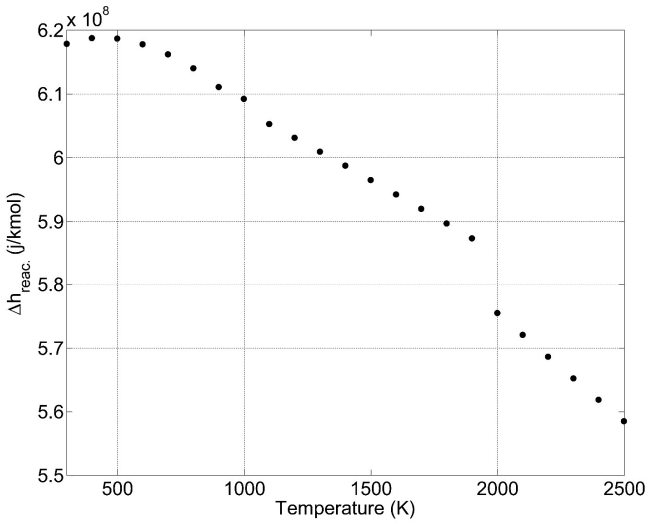


Fig. 4. The heat of the reaction [19]

5. Variations of the bed properties

Based on the nucleation and growth model, the existing SiO_2 in the solid bed is converted to SiC during the reaction time as below [1]:

$$\frac{dX}{dt} = \frac{k(1-X)}{-n\left[-\ln(1-X)\right]^{n-1}} \tag{10}$$

Therefore, during the reaction time, in addition to the variations in the temperature of this bed, the chemical composition of the bed is variated and some of the solid components convert to gaseous CO, which diffuses out the reactor bed and changes the porosity of this bed [2]. Attending to the existence of the values of the converted SiO_2 to SiC as a function of time (X), the values of the produced CO, removing carbon from the solid bed ($dX_C/dt = 3dX/dt$), and the value of decreasing of the solid bed volume due to removing of carbon ($X_C \rho_{eff} \left(W_C/\rho_C\right)(2\pi rldr)$) can be calculated, consequently. In a similar method, the value of decreasing this volume due to the conversion of SiO_2 particles to SiC and removal of O ($\left[w_{SiO_2}/\rho_{SiO_2} - \left(w_{SiO_2} M_{SiC}/(\rho_{SiC} M_{SiO_2})\right)\right](2\pi rlX\rho_{eff} dr)$ where w, M and l are weight fraction, molar weight and the length of cylindrical bad) can be calculated. Finally, assuming a constant structure for this solid bed, without breaking down due to increasing the porosity of this bed during the reaction time, the porosity of each calculation element of the reactor can be calculated $\varepsilon = \varepsilon_0 + V_d/V$ (ε is bed porosity and V is entered voltage to the core) using these calculated values of decreasing the solid bed volume. It should be noted that it is assumed that, the values of melted SiO_2 during this process are not high, else this melted phase can flow inside the porous bed and affects the porosity of different elements of this reactor. After obtaining the variation of the porosity of this bed, variations of the required properties of the solid bed can be calculated using the following equations:

$$\rho_{eff} = (1-\varepsilon)[(w_{C_i} - X_C w_{C_i})\rho_C + (w_{SiO_{2i}} - X w_{SiO_{2i}})\rho_{SiO_2} + (w_{SiC_i} - X w_{SiO_{2i}} \frac{M_{SiC}}{M_{SiO_2}})\rho_{SiC}] \tag{11}$$

$$C_{peff} = (1-\varepsilon)[(w_{C_i} - X_C w_{C_i})C_{pC} + (w_{SiO_{2i}} - X w_{SiO_{2i}})C_{pSiO_2} + (w_{SiC_i} - X w_{SiO_{2i}} \frac{M_{SiC}}{M_{SiO_2}})C_{pSiC}] \tag{12}$$

where ρ and C_p are density and heat capacity respectively. However, calculating the variation of the thermal conductivity of the bed (k_{eff}) is different. Since, the produced cylinder around the core of the reactor has a crystal network of SiC particles (formed nucleation of SiC on the surface of carbon has been grown and then connected to other SiC crystals [5]), attending to the super electrical and thermal conductivity property of SiC, therefore, the formed network of SiC crystals have the main rule in thermal conductivity of this section of the bed. Therefore, the effective thermal conductivity of the bed has been calculated as below:

$$k_{eff}=Xk_{SiC}+(1-X)(1-\varepsilon)[(w_{C_i}-X_C w_{C_i})k_C+(w_{SiO_{2i}}-Xw_{SiO_{2i}})k_{SiO_2}+(w_{SiC_i}-Xw_{SiO_{2i}}\frac{M_{SiC}}{M_{SiO_2}})k_{SiC}] \quad (13)$$

In these equations, the densities of the solid particles of SiO_2, C, and SiC are constants, but the heat capacity and thermal conductivity of these particles are functions of temperature [19, 24-27].

6. Mathematical model

The heat source of this reactor is a cylindrical graphite element at its core, i.e. the horizontal passing axes from the center of it. The heat losses from both sides of this element are considerable. In addition, the heat losses from both cylindrical cross surfaces of the reactor (at both the left and right sides of this reactor) and also the cylindrical side surface (ignoring the different condition of the top door of this reactor, which is open to the atmosphere for exiting the produced CO) have been considered in this model. Since the length of this reactor (l) is too longer than its inner radius (r_i), therefore, the temperature distribution along the length of this reactor is ignorable, in the comparison with its distribution in the direction of the reactor radius. In addition, it is assumed that the heat convection by the flow of CO inside the porosities of this bed is ignorable, in the comparison with the conduction and radiation of this energy inside the solid bed. Attending to the physical properties of the modeled solid contents of the reactor, it is assumed that the reactor's bed performs as a black body for absorbing and emitting the radiative thermal energy. Therefore, the entered radiative thermal energy to each one of the differential elements of the calculation domain (*i.e.* a cylindrical element with ID=2r) is equal to $(\sigma r T^4)_{in}$ and the exited value of this quantity from this cylindrical layer to the next layer (*i.e.* a cylindrical element with ID=2(r+dr)) is equal to $(\sigma r T^4)_{out}$. In addition, considering the physical properties of the SiC production in the Acheson reactor, there is no considerable fluid flow inside its solid bed. Therefore, this process has been simulated as a porous media of solid particles with a trapped gas phase in its porosity. Considering the T4 dependency of the radiative heat transfer rate to the temperature, in high-temperature layers of this reactor bed, the importance of the radiation heat transfer among these layers is much more importance than their conductive heat transfer. Therefore, the unsteady state equation of energy inside this bed can be calculated using the following equation.

$$(-k_{eff}r\frac{\partial T}{\partial r})_{\text{in}}+(\sigma r T^4)_{\text{in}}-(-k_{eff}r\frac{\partial T}{\partial r})_{\text{out}}-(\sigma r T^4)_{\text{out}}-(q_{react.}rdr)_{\text{C.V.}}$$
$$-(q_{melt.}rdr)_{\text{C.V.}}-(q_{loss.z}\frac{rdr}{l})_{\text{C.V.}}=[rdr\frac{\partial}{\partial t}(\rho_{eff}C_{peff}T)]_{\text{C.V.}} \quad (14)$$

where σ and T are Boltzmann constant and temperature. $q_{melt.}$ and $q_{react.}$ can be calculated at different temperatures using the presented Fig. 2 and Fig. 4. In this equation, the conduction and radiation of heat (assuming the black body property) inside the solid bed, heat losses from both cylindrical cross surfaces at both sides of the reactor (

$q_{loss.z} = 2(T - T_\infty) \Big/ \left[\frac{l_{iso}}{k_{iso}} + \frac{l_{steal}}{k_{steal}} + \frac{1}{h_{out.z}} \right]$), heat consumption of the endothermic chemical reaction, and the melting process, and also the accumulation of the energy have been considered. At the boundary of the solid bed with the graphite core of the reactor, the generated thermal energy in this core enters the solid bed. Attending to the dependency of the electrical resistance of the graphite core (R_{core}) to temperature [28] and the constant value of the entered voltage to this electrode (V_{core}), the rate of heat generation within this electrode using the entered electrical power ($P_{core} = V_{core}^2 / R_{core}$) is a function of its temperature. Of course, attending to free access of this electrode to the surface, the notable value of this generated power has been lost by the radiation mechanism from the left and right sides of this electrode at high temperatures, especially ($q_{loss.core} = 2\pi r_{core}^2 \sigma T_{core}^4$). This heat loss has been considered in the calculation of the entered thermal energy to the solid bed. At another boundary of this solid bed (the cylindrical side surface of this bed), heat conduction within the isolated and also steal layers, and heat convection in the air outside the reactor ($q_{loss.r} = r_i (T - T_\infty) \Big/ \left[\frac{l}{k_{iso}} \ln\left(\frac{r_i + l_{iso}}{r_i} \right) + \frac{l}{k_{steal}} \ln\left(\frac{r_i + l_{iso} + l_{steal}}{r_i + l_{iso}} \right) + \frac{1}{h_{out.r}(r_i + l_{iso} + l_{steal})} \right]$) have been considered in the model.

7. Numerical solution

Fig. 5 presents the developed solution procedure for this study. For numerical solving of the equations (10 and 14), these equations were discrete. The explicit and backward finite difference method was used for this purpose. First initial guesses (*i.e.* T=298K, X=0, X_C=0, and ε=0.39, attending to the real initial condition of the modeled process) have been chosen and then all of the dependent parameters to temperature were calculated and updated in a calculation loop. The governing equations were discretized explicitly and all gradient terms were approximated according to the Taylor series expansions backwardly. According to the explicit method the segregated approach is used for the calculation process and algorithm. Therefore, all variables are updated in every iteration of the calculation loop respectively. Therefore, these properties (such as ε, C_{peff}, k_{eff}, and ρ_{eff}) were calculated at the same time as the main variables of this model (T and X). The investigations for obtaining the convergence condition in this numerical solution, which had 1K accuracy for the calculated temperature, indicate that the convergence is reachable with $\frac{\Delta t}{\Delta r^2} \le 10^4$ sec/m^2. Therefore, this value was considered equal to 104sec/m^2 for a faster calculation. A homemade code was developed in the MATLAB software for parallel solving of this model using 4 cores of 7 cores processor (Intel Core i7-4.2GHz) of a computer with 57GB RAM and a 64bit operator. In this modeling, a uniform mesh, i.e. with a constant distance between its two nods in the radius direction, has been defined. Different calculation meshes were tested for mesh study. Fig. 6 shows the predictions of this model from the temperature of the core of the reactor at different times of the reaction using these meshes. As seen in this Figure, the meshes with Δr equal to 2.5mm and 5mm have similar predictions of the model. Therefore, model predictions for the defined meshes with $\Delta r \ge 2.5$mm are mesh-independent. Attending to the lower calculation time of the mesh with Δr=5mm ($t_{calculated}$=16588s), this mesh has been selected for further calculations. According to Fig. 6 increasing the mesh density enhanced core temperature illustration. dr=5mm has more sensitivity in front of core temperature without any fluctuation than dr=2.5mm. Consequently, mesh sizes were adjusted based on the dr=5mm.

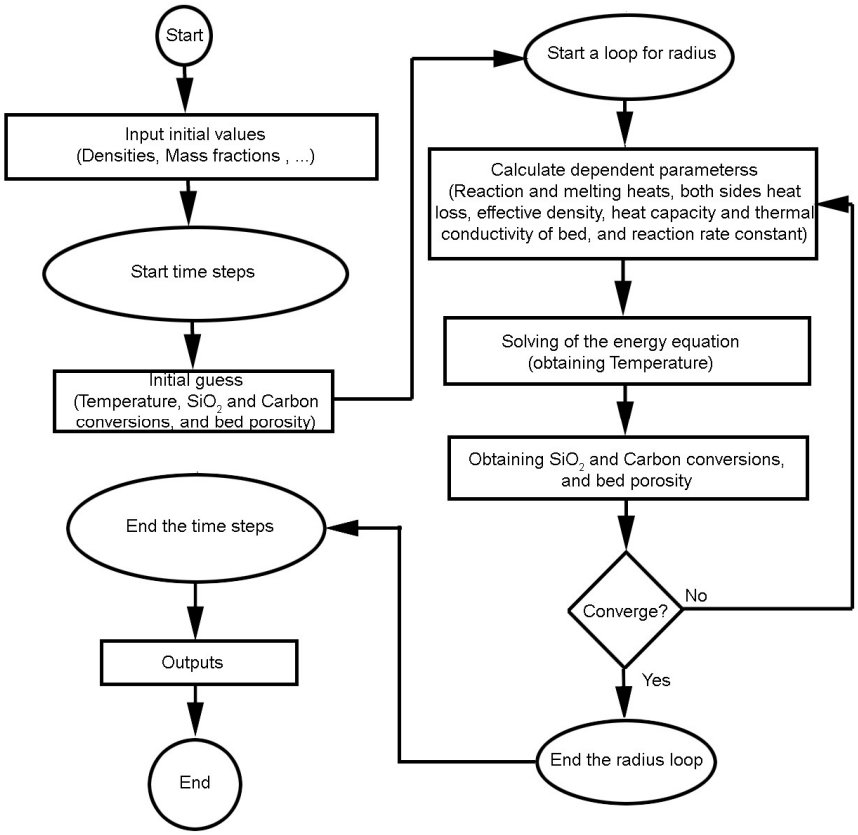


Fig. 5. Solution procedure

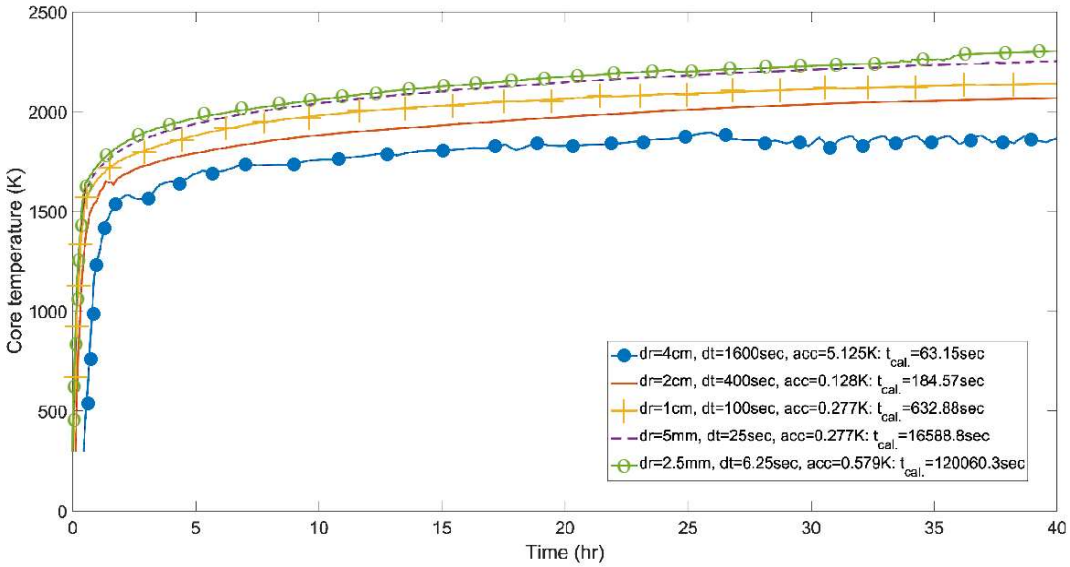


Fig. 6. Mesh study results

8. Results and discussion

Based on the available previous empirical data from the performance of mentioned reactor with the given properties in Table 1 reactor, the following predicted values by the model can be validated using these data: Temperature

variations of the core in the reaction duration; Temperature variations of a certain point of the solid bed, which was located on the outer surface of the produced SiC cylinder at the end of the reaction (after 40 hr), as a function of time Final porosity of the bed after 40hr; Value of the produced SiC at the end of the process.

Table 1. Properties of the modeled industrial reactor [1,15]

Parameter	Value
Time	40 hr
Electrode radius	84.857 mm
Reactor inner radius	1634.648 mm
Reactor inner length	9.14 m
The initial weight of cock	36840 kg
The initial weight of silica	58160 kg
The initial weight of silicon carbide	25253 kg
Power energy input	85 MW.hr
Initial porosity	0.39
Isolation thickness	10 cm
Steal thickness	1 cm
Initial temperature	298 K
Final porosity	0.69
The final radius of the produced SiC cylinder	130 cm
The percentage of the produced SiC	9%
The final temperature of the core	2037 K
The final temperature at the cylindrical side surface of the produced cylinder of SiC	1702 K

Fig. 7 illustrates the predictions of the model for the final conversion (after 40hr) of SiO_2 to SiC in different radiuses of the reactor. Based on the presented empirical value for the quality of the final production of SiC in this reactor, the formed cylinder of SiC around the core of the reactor has more than 96% SiC.

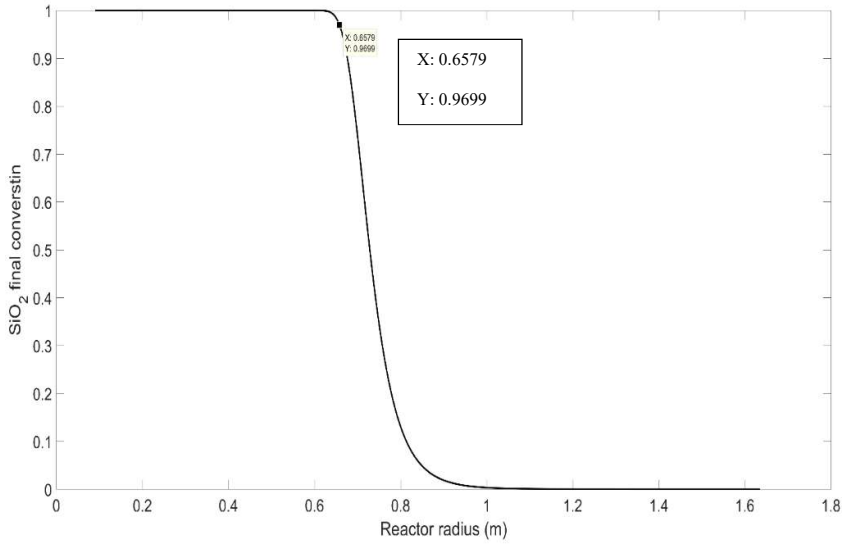


Fig. 7. Predictions of the model for the final conversion of SiO_2 to SiC

As seen in this Figure, the radiuses less than 0.658m inside this reactor have final conversions of more than 96%. Therefore, the final cylinder of the produced SiC in this reactor has a 131.58cm diameter, which is too close to the presented empirical value for this parameter (130cm [15]). Fig. 8 shows a contour of the predicted values for local SiO_2 conversion inside the reactor during the reaction time.

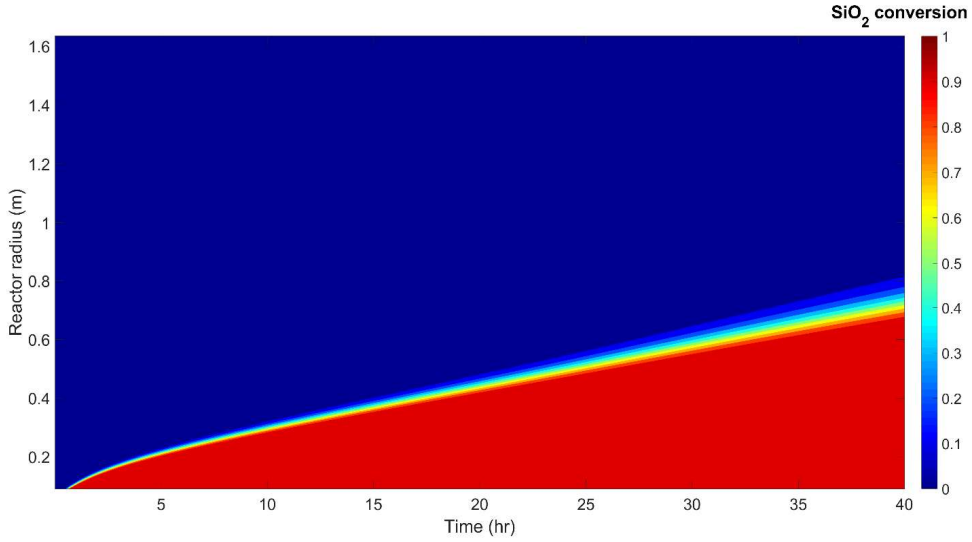


Fig. 8. The contour of the predicted values for local SiO_2 conversion

Fig. 9 shows the predictions of the model for temperatures of the core and the mentioned located point at the outer surface of the produced SiC cylinder at the end of the reaction (at r=0.658mm), as functions of reaction time. Empirical values of these temperatures have also been presented in this Figure for validation of the model predictions [1]. As seen in this Figure, the presented model has acceptable predictions for these parameters.

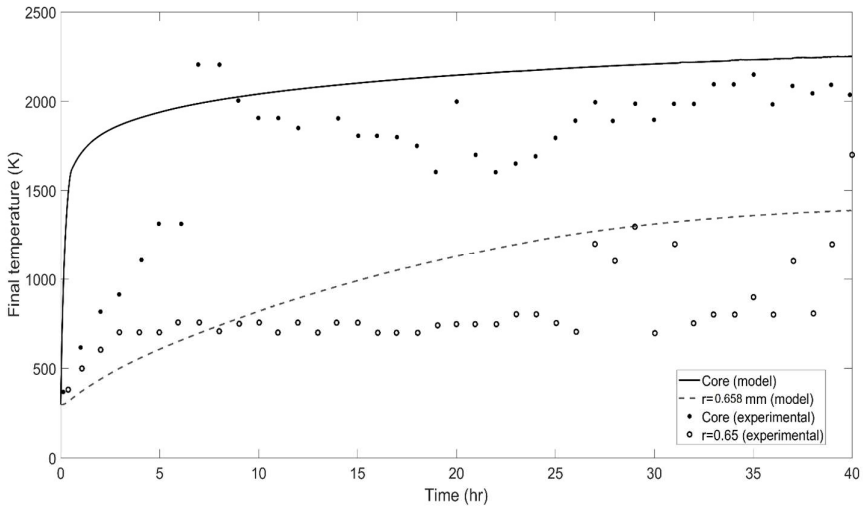


Fig. 9. Predictions of the model for temperatures of the core and the outer surface of the produced SiC cylinder at the end of the reaction

Fig. 10 shows a contour for the predicted local values of the bed temperature during the reaction time. It should be noted the compared empirical data was on an industrial scale, which had low-quality of initial materials that caused the unpredictable effects of these impurities in the reaction process. On the other hand, some random effects, such as instantaneous displacements of the solid bed by the movement of exiting CO gas from this bed, caused some instantaneous variations of the measured temperature in the rector. Therefore, the fluctuations of the measured temperature in this reactor were inevitable, which was not predictable by the present theoretical model. Nevertheless,

the overall changes in the measured temperature within the reactor and also their final values have been predicted by the model.

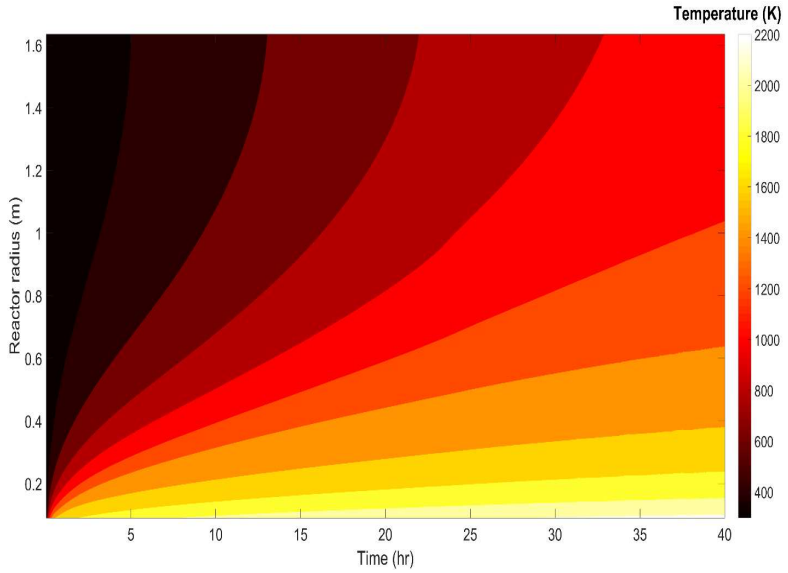


Fig. 10. The contour of the predicted local values of the bed temperature

Fig. 11 shows a contour for the predicted local values of the bed porosity during the reaction time. Fig. 12 also shows the model predictions for the melted SiO_2 in this bed. This Figure approves our assumptions that this melting rate is low enough and has no considerable effect on the bed porosity. The calculated average value of the final porosity of different radiuses of this bed is 0.56, which is close to the measured value for this parameter, *i.e.* 0.62 [15].

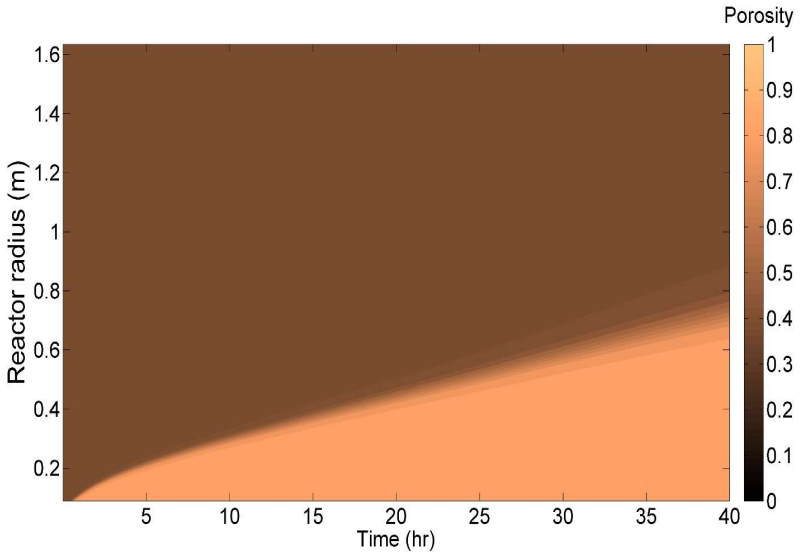


Fig. 11. The contour of the predicted local values of the bed porosity

This predicted value has less than 10% relative error from the measured empirical data, which is acceptable attending to the complexity of this phenomenon and the various effects of unpredictable, such as impurities, particle size distribution, different particle shapes, inhomogeneous bed, and extra. Considering the calculated values for the porosity of the final produced cylinder of SiC (with 131.58cm diameter), calculating the weight of this cylinder and dividing this weight by the weight of the initial materials of the bed, the percentage of SiC production can be

calculated. This calculated value is 8.16%, which is close to its empirical value of 9% (see reference [15]). This predicted value also has less than a 10% relative error from the measured empirical data.

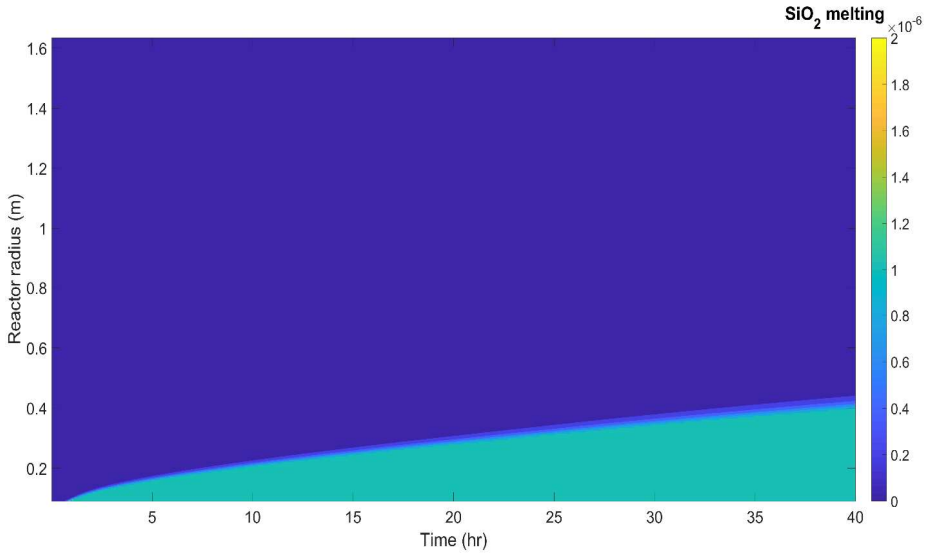


Fig. 12. The model predictions for the melted SiO_2 in this bed

Fig. 13 shows the order of the heat loss from both sides of this reactor. The order of this heat loss is in the range of the lateral surface heat loss of this industrial reactor. Therefore, the value of this heat loss is considerable and it is not possible to neglect its overall effects. It is also observed that, in the initial hours of this process, $q_{loss,z}$ is more than $q_{loss,r}$, and vice versa in the final hours of this process. The reason is that $q_{loss,z}$ contains the heat loss of different radiuses of the reactor, and some of these radiuses have considerable temperatures attending to their distances from the reactor core, but, $q_{loss,r}$ only affects by the temperature of the outer layer is of the solid bed, which has low temperatures in initial times of the process.

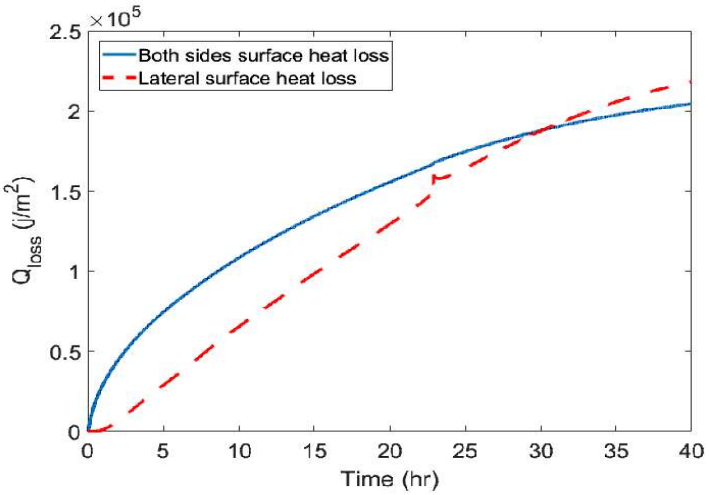


Fig. 13. The model predictions for heat losses from both sides and also the lateral surfaces of the reactor

9. Conclusion

In the presented study, a one-dimensional unsteady-state model was developed to model the Acheson reactor for producing SiC. The mechanisms of the melting of SiO_2 and converting this component to SiC were investigated. The obtained mechanisms were utilized in the developed model. The properties of the bed and the core of the reactor were varied by the temperature and reaction time. The explicit and backward finite difference method was used for the numerical solving of this model. The prediction of this model was validated using the empirical data of the temperature variations of the core and a certain point of the solid bed in the reaction duration, the final porosity of the bed, and the value of the produced SiC at the end of the process.

Nomenclature

$C_{P_{eff}}$	Effective heat capacity of the bed (*J/kmol/K*)	$Q_{loss.z}$	Heat loss from the left and right cylindrical cross surfaces of the reactor (J/m^2)
C_{P_C}	Heat capacity of carbon (*J/kmol/K*)	$Q_{loss.r}$	Heat loss from the cylindrical side surface of the reactor (J/m^2)
$C_{P_{SiC}}$	Heat capacity of SiC (*J/kmol/K*)	$q_{melt.}$	Heat consumption by SiO_2 melting(J/m^3)
$C_{P_{SiO_2}}$	Heat capacity of SiO_2 (*J/kmol/K*)	$q_{reac.}$	Heat consumption by the reaction (J/m^3)
E	The activation energy (*J/kmol*)	R_{core}	The electrical resistance of the graphite core (Ω)
$h_{loss.r}$	Convection heat coefficient of air around the cylindrical side surface of the reactor	r	Coordination in the radius of the cylindrical bad (*m*)
$h_{loss.z}$	Convection heat coefficient of air beside the cylindrical cross surfaces of the reactor	r_{core}	The radius of the core (*m*)
k	The reaction rate constant (*1/sec*)	r_i	The inner diameter of the reactor (*m*)
k_0	Pre-exponential constant (*1/sec*)	V_{core}	Entered voltage to the core electrode (*volt*)
k_{eff}	Effective thermal conduction of the bed (*W/m/K*)	w_C	The weight fraction of carbon in the bed
k_C	Thermal conduction of carbon (*W/m/K*)	w_{C_i}	The initial weight fraction of carbon in the bed
k_{iso}	Thermal conduction of isolation layer (*W/m/K*)	w_{SiC}	The weight fraction of SiC in the bed
k_{steal}	Thermal conduction of steal (*W/m/K*)	w_{SiC_i}	The initial weight fraction of SiC in the bed
k_{SiC}	Thermal conduction of SiC (*W/m/K*)	w_{SiO_2}	The weight fraction of SiO_2 in the bed
k_{SiO_2}	Thermal conduction of SiO_2 (*W/m/K*)	$w_{SiO_{2i}}$	The initial weight fraction of SiO_2 in the bed
l	Length of the cylindrical bad (*m*)	X	SiO_2 conversion
l_{iso}	Isolation thickness (*m*)	X_C	Carbon conversion
l_{steal}	Steal thickness (*m*)	ε	Bed porosity
M_C	The molecular weight of carbon (*kmol/kg*)	ρ_{eff}	Effective density of the med ($kmol/m^3$)
M_{SiC}	The molecular weight of SiC (*kmol/kg*)	ρ_C	The density of carbon ($kmol/m^3$)
M_{SiO_2}	The molecular weight of SiO_2 (*kmol/kg*)	ρ_{SiC}	The density of SiC ($kmol/m^3$)
n	Reaction order attending to SiO_2 concentration	ρ_{SiO_2}	The density of SiO_2 ($kmol/m^3$)
P_{core}	entered electrical power to the core of the reactor (*Watt*)	σ	Boltzmann constant

Conflict of interest

The authors declare that there is no conflict of interest regarding the publication of this article.

Funding

This research received no specific grant from any funding agency in the public, commercial, or not-for-profit sectors.

References

[1] Gupta, G.S., Vasanth Kumar, P., Rudolph, V.R. and Gupta, M., 2001. Heat-transfer model for the acheson process. Metallurgical and Materials Transactions A, 32(6), 1301-1308. https://doi.org/10.1007/s11661-001-0220-9
[2] Carbide, N., 1997. Boride materials-synthesis and processing, edited by Aw Weimer. Chapman and Hall, London.
[3] Acheson, E.G., 1893. Carborundum: Its history, manufacture and uses. Journal of the Franklin Institute, 136(3), 194-203. https://doi.org/10.1016/0016-0032(93)90311-H
[4] Searcy, A.W. 1963. High-temperature reactions. Survey of Progress in Chemistry, 1, 35-79. https://doi.org/10.1016/B978-1-4832-0003-3.50007-7
[5] Węgrzyn, J., 2015. Comparison of mass loss rate in reaction of silica with carbon from different investigation results. Metalurgija, 54(3), 579-582.
[6] Weimer, A.W., Nilsen, K.J., Cochran, G.A. and Roach, R.P., 1993. Kinetics of carbothermal reduction synthesis of beta silicon carbide. AIChE Journal, 39(3), 493-503. https://doi.org/10.1002/aic.690390311
[7] Kennedy, P. and North, B., 1983. Proceedings of the British Ceramic Society. Stoke-on-Trent: British Ceramic Society.
[8] Kevorkijan, V.M., Komac, M. and Kolar, D., 1989. Ceramic powder processing science. Koln: Deutsche Keramische Gesellschaft, 327-333.
[9] Kikuchi, T., Kurosawa, T. and Yagihashi, T., 1969. Carbothermic Reduction of Silica (Studies on the Production of Crude Aluminium Alloy by the Direct Reduction of Aluminous Ores (III). Transactions of the Japan Institute of Metals, 10(2), 140-146. https://doi.org/10.2320/matertrans1960.10.140
[10] Shimoo, T. and Mizutaki, F., 1989. Effect of particle-size of carbon on the reduction rate of powdered SiO_2-C mixtures., Journal of the Japan Institute of Metals, 53(8), 838-839. https://doi.org/10.2320/jinstmet1952.53.8_838
[11] Ono, K. and Kurachi, Y., 1991. Kinetic studies on β-SiC formation from homogeneous precursors. Journal of materials science, 26(2), 388-392. https://doi.org/10.1007/BF00576531
[12] Van Dijen, F.K. and Metselaar, R., 1991. The chemistry of the carbothermal synthesis of β-SiC: Reaction mechanism, reaction rate and grain growth. Journal of the European Ceramic Society, 7(3), 177-184. https://doi.org/10.1016/0955-2219(91)90035-X
[13] Krishnarao, R.V. and Mahajan, Y.R., 1996. Formation of SiC whiskers from raw rice husks in argon atmosphere. Ceramics international, 22(5), 353-358. https://doi.org/10.1016/0272-8842(95)00084-4
[14] Shimoo, T., Mizutaki, F., Ando, S. and Kimura, H., 1988. Mechanism of formation of SiC by reduction of SiO with graphite and CO. Nippon Kinzoku Gakkaishi;(Japan), 52(3).
[15] Kumar, P.V. and Gupta, G.S., 2002. Study of formation of silicon carbide in the Acheson process. Steel research, 73(2), 31-38. https://doi.org/10.1002/srin.200200170
[16] Nagamori, M., Leblanc, R. and Courtemanche, R., 1993. Power consumption in the Acheson process for producing SiC. Developments and Applications of Ceramics and New Metal Alloys, 301-312.
[17] Derevyanko, I.V. and Zhadanos, A.V., 2010. Mathematical modeling of heat power processes of silicium carbide production in acheson furnace. Metallurgical and Mining Industry, 2(5), 331.
[18] Ainslie, N.G., Mackenzie, J.D. and Turnbull, D., 1961. Melting kinetics of quartz and cristobalite. The Journal of Physical Chemistry, 65(10), 1718-1724. https://doi.org/10.1021/j100827a012
[19] Roine, A., 2006. HSC 6.0 Chemistry. Chemical reactions and Equilibrium software with extensive thermochemical database and Flowsheet simulation. Pori: Outokumpu research Oy.
[20] Filsinger, D.H. and Bourrie, D.B., 1990. Silica to silicon: key carbothermic reactions and kinetics. Journal of the American Ceramic Society, 73(6), 1726-1732. https://doi.org/10.1111/j.1151-2916.1990.tb09820.x
[21] Abolpour, B., Afsahi, M.M. and Azizkarimi, M., 2018. Reduction kinetics of magnetite concentrate particles by carbon monoxide. Mineral Processing and Extractive Metallurgy, 127(1), 29-39. https://doi.org/10.1080/03719553.2016.1277
[22] Abolpour, B., Afsahi, M.M. and Azizkarimi, M., 2021. Hydrogen reduction of magnetite concentrate particles. Mineral Processing and Extractive Metallurgy, 130(1), 59-72. https://doi.org/10.1080/25726641.2018.1521576
[23] Nomura, Y., Nakagawa, H., Maeda, T., Nishioka, K. and Shimizu, M., 2005. Rapid reduction of fine iron ore transported with CH4 gas. Tetsu-to-hagane, 91(6), 521-527. https://doi.org/10.2355/tetsutohagane1955.91.6_521
[24] Perry, R.H., Green, D.W. and Maloney, J.O., 1997. Perry's handbook of chemical engineering. Perry's Handbook of Chemical Engineering.
[25] Kaye, G.W.C. and Laby, T.H., 1966. Tables of physical and chemical constants and some mathematical functions.
[26] Touloukian, Y.S. and Makita, T., 1970. Thermophysical properties of matter-the TPRC data series. volume 6. specific heat-nonmetallic liquids and gases. Thermophysical and electronic properties information analysis center lafayette in.
[27] Harris, G.L., 1995. Properties of silicon carbide, INSPEC. The Institution of Electrical Engineers, London, 5.
[28] Jiang, S., Horn, T.J. and Dhir, V.K., 2000. Numerical analysis of a radiant heat flux calibration system. International journal of thermophysics, 21(4), 941-963. https://doi.org/10.1023/A:1006622526578
[29] Holman, J.P., 1997. Heat transfer, 8th Edition. New York.
[30] Abolpour, B., 2021, Modeling of oxidation of UO2 pellets. Annals of Nuclear Energy, 151, 107955. https://doi.org/10.1016/j.anucene.2020.107955
[31] Abolpour, B. and R. Shamsoddini, 2020, Mechanism of reaction of silica and carbon for producing silicon carbide. Progress in Reaction Kinetics and Mechanism, 45. https://doi.org/10.1177/1468678319891416
[32] Gupta, G.S., Raj, P. and Tiwari, K., 2019. An Analysis of Heat Distribution in the Production of SiC Process. Procedia Manufacturing, 30, 64-70. https://doi.org/10.1016/j.promfg.2019.02.010

[33] Alweendo, S.T., Johnson, O.T., Shongwe, M.B., Kavishe, F.P. and Borode, J.O., 2019. Synthesis, optimization and characterization of silicon carbide (SiC) from rice husk. Procedia Manufacturing, 35, 962-967. https://doi.org/10.1016/j.promfg.2019.06.042
[34] Feng, D., Qin, Z., Ren, Q., Sun, S., Xia, Q., Ru, H., Wang, W., Ren, S. and Zhang, C., 2022. Occurrence forms of major impurity elements in silicon carbide. Ceramics International, 48(1), 205-211. https://doi.org/10.1016/j.ceramint.2021.09.095
[35] Matizamhuka, W.R., 2019. Gas transport mechanisms and the behaviour of impurities in the Acheson furnace for the production of silicon carbide. Heliyon, 5(4), e01535. https://doi.org/10.1016/j.heliyon.2019.e01535
[36] Raj, P. and Gupta, G.S., 2020. Temperature measurements in a laboratory scale furnace for manufacturing of silicon carbide through Acheson process. Measurement, 151, 107131. https://doi.org/10.1016/j.measurement.2019.107131
[37] Raj, P., Gupta, G.S. and Rudolph, V., 2020. Silicon carbide formation by carbothermal reduction in the Acheson process: A hot model study. Thermochimica Acta, 687, 178577. https://doi.org/10.1016/j.tca.2020.178577
[38] Hossain, S.T., Johra, F.T. and Jung, W.G., 2018. Fabrication of silicon carbide from recycled silicon wafer cutting sludge and its purification. Applied Sciences, 8(10), 1841. https://doi.org/10.3390/app8101841
[39] Rao, M.P.L.N., Gupta, G.S., Manjunath, P., Kumar, S., Suri, A.K., Krishnamurthy, N., Subramanian, C., 2009. Core temperature measurement in carbothermal reduction processes. Thermochimica Acta, 482(1-2), 66-71. https://doi.org/10.1016/j.tca.2008.10.016